

BENCHMARK VERCORS 2022: BLIND PREDICTION OF TIME-DEPENDENT BEHAVIOR OF CONCRETE CONTAINMENT BUILDING WITH LOW AND HIGH-FIDELITY MODELS

ŠTĚPÁN KRÁTKÝ*, PETR HAVLÁSEK

Czech Technical University in Prague, Faculty of Civil Engineering, Department of Mechanics, Thákurova 7, 166 29 Prague 6, Czech Republic

* corresponding author: stepan.kratky@fsv.cvut.cz

ABSTRACT. The VERCORS program aims to acquire an extensive experimental dataset collected to provide a solid basis for numerical modeling of concrete containment buildings (CCBs). In order to cover the entire life-span of a real containment, the measurements are done on $3\times$ smaller mock-up which leads to 9-fold acceleration of all processes related to drying. The goal for the participants of the third VERCORS benchmark was to predict the behaviour of the CCB based on standard laboratory measurements on VERCORS concrete. The previous paper [1] presented the calibration procedure of material models for moisture transport and time-dependent behavior of concrete and summarized the results obtained with a computationally efficient low-fidelity model (LFM). The present paper compares the responses of the LFM and a high-fidelity model (HFM) with a detailed geometry of the entire containment and presents a comparison with the experimental data collected over the last 8 years on the VERCORS mockup.

KEYWORDS: Concrete, creep, shrinkage, drying, cyclic temperature, modeling.

1. INTRODUCTION

In order to prolong the lifespan of concrete containment buildings of nuclear reactors by 50 %, detailed knowledge of their time-dependent behaviour is essential. This implies the ability to accurately predict the evolution of various quantities over 60 years. Such a task can be accomplished by computational modeling with advanced constitutive models. The main task of the first phase of the VERCORS 3rd benchmark was to predict the behavior of the concrete containment building (CCB) depicted on Figure 1, in particular the evolution of strain, displacement and relative humidity at prescribed locations. For a smoother evaluation of the benchmark and simpler comparison of the results among the participants, the organizers provided a detailed finite element mesh of the CCB.

This paper is organized as follows. The main results of the previous paper [1] are summarized first. Next, the low- and high-fidelity numerical models (LFM and HFM) are described and their features are presented. Finally, the responses of LFM and HFM are compared with the experimental response.

2. PREVIOUS OUTCOMES

2.1. LABORATORY EXPERIMENTS

The provided dataset constitutes from the results of conventional short-term measurements (mean uniaxial compressive strength $f_{cm} = 48.7\text{ MPa}$, Young's modulus $E = 34.3\text{ GPa}$, uniaxial tensile strength $f_t = 4.4\text{ MPa}$) and the following long-term experiments:

- Basic creep and autogenous shrinkage,

- total creep and drying shrinkage at relative humidity of the environment $h_{env} = 0.5$,
- moisture loss,
- porosity and aging sorption isotherm.

Every experiment in this list was conducted under both room (20 °C) and elevated (40 °C) temperature. This data set was used for calibration of constitutive models.

2.2. FINITE ELEMENT MODELING

OOFEM [3] solver was used to run all numerical simulations. A weakly coupled computational approach was adopted to model the influence of temperature and relative humidity on the structural response. Moreover, to further simplify the problem, no cross-coupling between the heat and moisture transport subproblems was assumed in the blind stage of the benchmark. This is partially due to the absence of relevant data.

2.3. CALIBRATION OF MATERIAL MODELS

The constitutive models for heat and moisture transport (Bažant-Najjar model [4]) and time-dependent behavior of concrete (modified MPS model [5]) were calibrated using axis-symmetric models of laboratory specimens. The experimental data sets were provided by EDF (Électricité de France) at the beginning of the benchmark. Successful calibration of the constitutive models is demonstrated by excellent fits of the data and can be found in the final thesis of the first author [6].

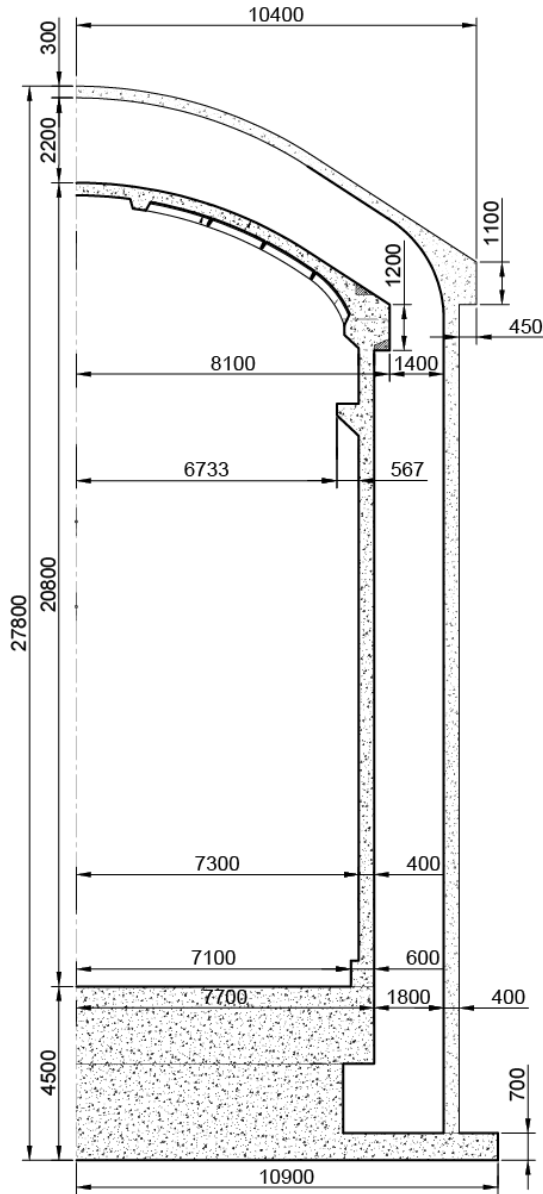


FIGURE 1. Section of the CCB VERCORS mock-up [2], dimensions in [mm].

The calibration procedure is briefly outlined in the following sections and the identified values of material parameters for the Vercors concrete are listed in Tables 1 and 2.

2.3.1. BASIC CREEP AND AUTOGENOUS SHRINKAGE

Under hygrally sealed conditions and at constant room temperature, the MPS model reduces to the basic creep compliance function of the B3 [7] model whose parameters q_1 – q_4 were initially estimated from the composition of the concrete mixture. These parameters were slightly adjusted to obtain a more accurate fit of the experimental data.

The measured strain in the creep experiment was compensated for the autogenous shrinkage measured on a companion specimen. Since the experiment began at the age of 90 days, the recorded (incremental) value of autogenous shrinkage was very small, $\approx 50 \times 10^{-6}$.

Parameter	Value
q_1	$9.0 \times 10^{-6} \text{ MPa}^{-1}$
q_2	$70.0 \times 10^{-6} \text{ MPa}^{-1}$
q_3	$25.0 \times 10^{-6} \text{ MPa}^{-1}$
q_4	$6.0 \times 10^{-6} \text{ MPa}^{-1}$
k_{sh}	1.0×10^{-3}
k_3	10
k_{Tm}	6.5

TABLE 1. Identified parameters of the MPS material model.

Parameter	Value
C_1	$28.2 \text{ mm}^2 \cdot \text{day}^{-1}$
α_0	0.055
h_c	0.7
n	10
f	$1.08 \text{ mm} \cdot \text{day}^{-1}$

TABLE 2. Identified parameters of the material model Bažant–Najjar for moisture diffusion.

Autogenous shrinkage per se was not considered in the analysis.

2.3.2. DRYING AND DRYING SHRINKAGE

Parameters of the Bažant–Najjar model for moisture diffusion [4] were determined by hand fitting and were calibrated simultaneously with the parameter k_{sh} of the MPS model which links the rates of axial drying shrinkage and relative humidity. The response of the models was checked against the measured evolution of drying shrinkage and moisture loss at room temperature. To back-calculate the moisture loss from the relative humidity, the moisture capacity was set to 130 kg/m^3 which approximately corresponds to the slope of the measured desorption isotherm.

2.3.3. DRYING CREEP

Parameters for the drying creep, creep at elevated temperature, and transitional thermal creep were determined last. Drying creep is controlled chiefly via parameter k_3 . The experimental data on cylinders allowed to identify parameter k_{Tm} which is responsible for the creep rate at elevated temperature. However, under temperature cycles this value would have caused overestimated compliance. Unfortunately, the experimental data set did not comprise sufficient information to allow for calibration of the last parameter which damps concrete creep at subsequent thermal cycles, k_{Tc} .

2.3.4. HEAT TRANSFER

There were no relevant data for the identification of parameters related to heat conduction; therefore, typical values for concrete were adopted: heat capacity $c = 1000 \text{ J} \cdot \text{kg}^{-1} \cdot \text{K}^{-1}$, heat conductivity $k = 1.7 \text{ W} \cdot \text{m}^{-1} \cdot \text{K}^{-1}$, and surface factor $a = 8 \text{ W} \cdot \text{m}^{-2} \cdot \text{K}^{-1}$.

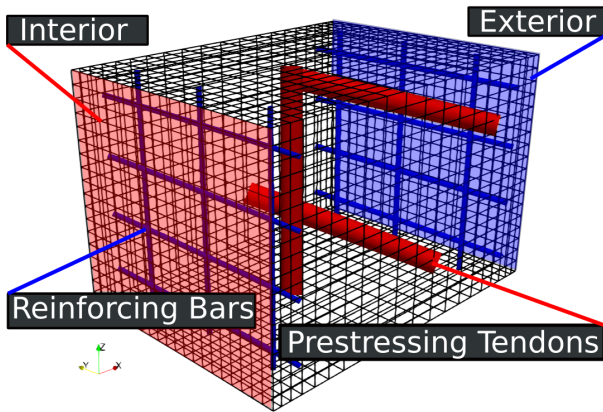


FIGURE 2. LFM – structural model.

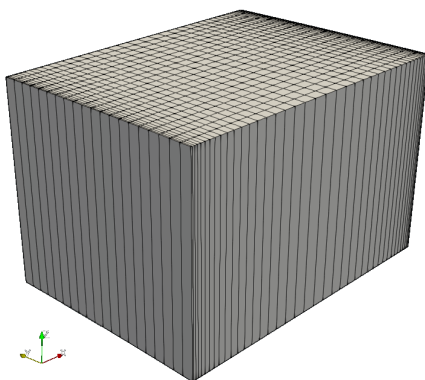


FIGURE 3. LFM – moisture transport model.

2.3.5. DAMAGE

Except for the pressure tests, the stress state in the CCB is chiefly biaxial compression in plane of the cylinder and dome. The out-of-plane stress is far below the strength limit. Since the benchmark results do not cover places with significant stress concentrations, the nonlinear behavior does not need to be considered. For this reason, concrete damage (neither compressive nor tensile) was not considered in the first stage of the benchmark.

2.4. LOW-FIDELITY MODEL

The enormous computational demands of the high-fidelity model made it impossible to tune up the boundary conditions and the remaining parameters related to transient thermal creep, which could not be identified from the experimental data. Therefore, a computationally efficient numerical model was developed to verify the response to the ambient conditions. The resulting low-fidelity model represents a small segment of the wall in the mid-height of the CCB to eliminate the interaction with more rigid parts of the structure (foundation slab and dome stiffener). The finite element meshes for the individual subproblems – structural analysis, moisture transport, and heat transfer – are shown in Figures 2, 3 and 4. The dimensions of the computational models are derived

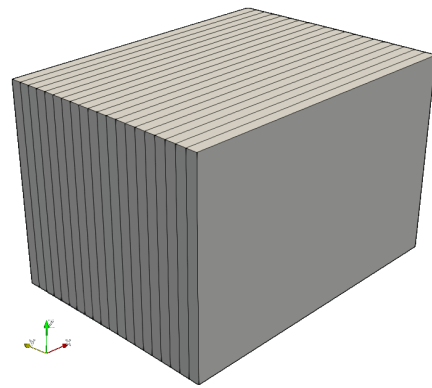


FIGURE 4. LFM – heat transfer model.

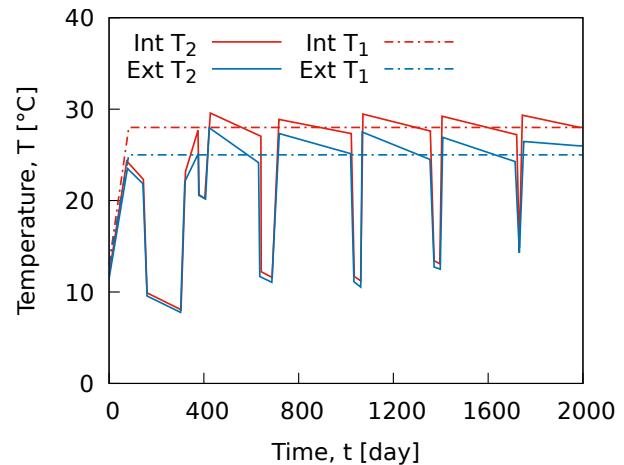


FIGURE 5. Ambient conditions – temperature prescribed on the inner and outer faces of the concrete wall.

from the spacing of the prestressing tendons in the vertical and circumferential directions.

2.5. RESULTS

A comprehensive description and discussion of the results can be found in the previous paper [1]. The most significant discrepancy in the structural behavior was associated with the response to the (simplified) ambient conditions, in particular temperature (program T₂ in Figure 5). Although a higher creep rate can be anticipated under cyclic temperature, the resulting strains were several times higher than under T₁ program with bilinear temperature history. This response was considered as unrealistic. To damp the excessive sensitivity to subsequent temperature cycles, the parameter k_{Tc} was introduced and set to $k_{Tm}/20$.

3. HIGH-FIDELITY MODEL

In order to obtain compatible results with the benchmark specifications, a full-lifespan simulation was finally run on the HFM. To detect unintentional mistakes which are likely to be made when modeling large structures with complex boundary conditions, the similarity of the HFM response at the mid-height was subsequently cross-checked with the LFM.

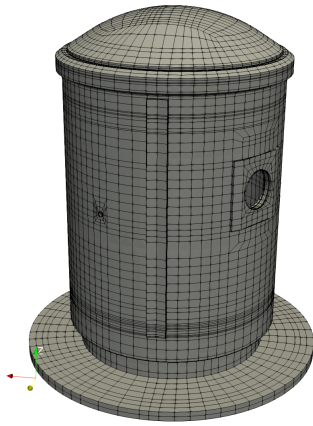


FIGURE 6. HFM – structural model of concrete containment building.

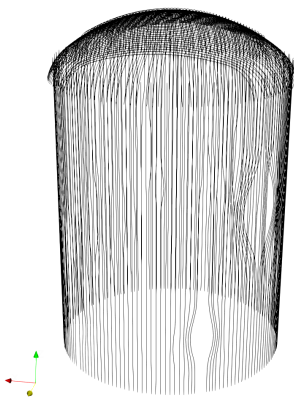


FIGURE 7. HFM – structural model of vertical and dome tendons.

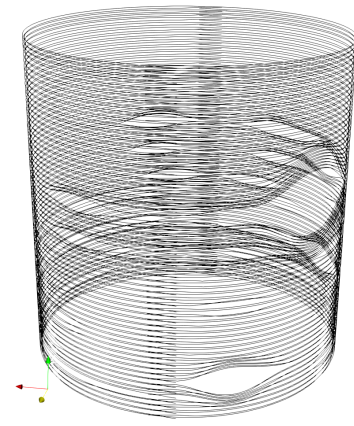


FIGURE 8. HFM – structural model of hoop tendons.

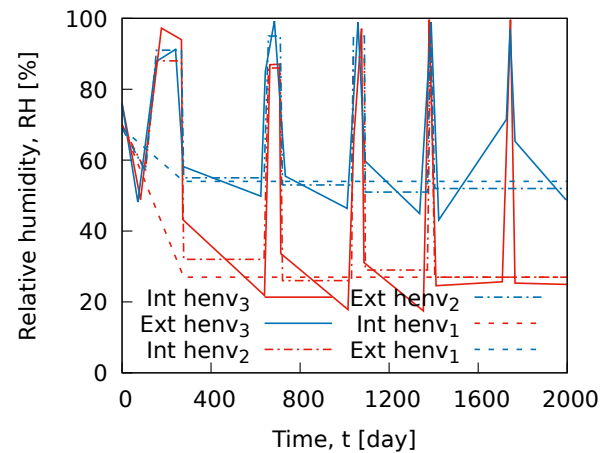


FIGURE 9. Ambient conditions – relative humidity prescribed on the inner and outer faces of the concrete wall.

3.1. STRUCTURAL MODEL

Structural HFM (Figures 6, 7 and 8) with 635 328 degrees of freedom is composed of the concrete body (quadratic brick elements) and prestressing tendons (linear truss elements); conventional concrete reinforcement is neglected due to its low influence on the global behavior. Fully fixed boundary conditions are assigned to the bottom face of the substructure. This simplification was acceptable because of the extreme stiffness of the substructure in comparison with the superstructure. As no specific prestressing schedule was provided, prestressing of all tendons was set to day 278+45 of the simulation. The value of eigenstrain assigned to every tendon is constant over its length and thus does not reflect the direction of prestressing; the prestress losses due to friction are evaluated according to Eurocode 2. Due to the instantaneous deformation of the concrete structure, even the initial distribution of prestress is not uniform. Gradual prestress relaxation is described by the *fib* Model Code 2010/Eurocode 2 (Annex D) approach which uses the concept of equivalent time. The material constants adopted comply with Class 2 reinforcement (wire or strands with low relaxation). Characteristic strength is defined as 1870 MPa and the Young modulus is 190 GPa. The effects of elevated temperature or tem-

perature fluctuations on the relaxation rate are not considered.

The periods with the increased value of inner overpressure, which would have led to the development of tensile cracks, are not considered in the analysis as the influence on the long-term behavior is negligible because the cracks completely close once the overpressure vanishes.

3.2. MOISTURE AND HEAT TRANSFER

Models for moisture and heat transfer with 1061 450 degrees of freedom represent the concrete body discretized by linear brick elements. The boundary conditions are assigned to the inner and outer face of CCB.

Similarly to LFM, the real history of ambient conditions provided by EDF, which was measured on VERCORS mock-up, was simplified into several programs with different complexity. Unrealistic response of the constitutive model to cyclic temperature was prevented by the parameter k_{Tc} which in turn allowed to adopt more complex history of ambient temperature (Int/Ext T_2 in Figure 5) and thus to get closer to the actual measurements. Ambient relative humidity was defined by henv₃ shown in Figure 9.

Analysis	HFM Linear	LFM Linear
DOF (SM)	635 328	26 166
Memory consumption	34 GB	-
CPU	i9-11900 RL	AMD 5 3600
CPU threads used	8	1
Time steps	382	382
Time consumption (RT)	31.5 hours	0.7 hours

TABLE 3. Comparison of the characteristics of HFM and LFM.

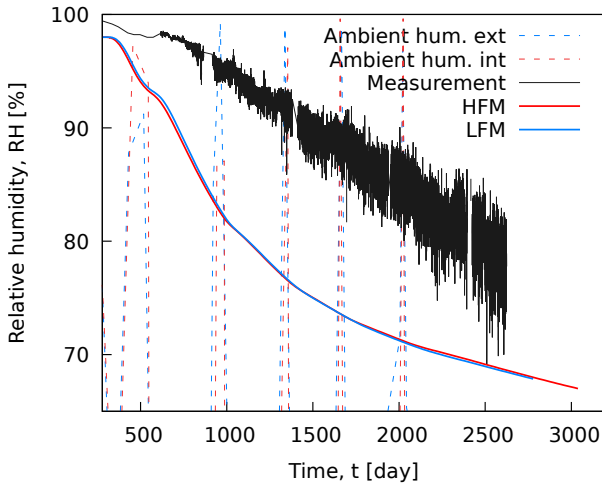


FIGURE 10. Evolution of relative humidity: LFM, HFM and experiment.

4. RESULTS AND DISCUSSION

The original intention of the authors was not only to thoroughly evaluate the behaviour of the CCB but also to use the measurements to improve the behavior of the constitutive model of concrete and possibly also steel relaxation. At the very beginning of the benchmark, the participants were promised that after the initial blind stage of the benchmark, they would be granted full access to the Cheops database with detailed information including hundreds of strain, displacement, humidity, and temperature sensors. Unfortunately, after months of work of the present authors, the organizers revealed data on a very limited fraction of the structure referred to as PACAR area with dimensions 2×2 meters approximately in the middle of the height of the cylinder whose response should be in a good agreement with the LFM model. Data of relative humidity were available for a single sensor, which can neither support the credibility of the computational models nor it can provide confidence about the accuracy of the experimental data. Comparison of several characteristics of LFM and HFM models is summarized in Table 3.

All future goals of further studies on nonlinear models, evolution of damage, and the behaviour under increased pressure were thus dropped as there is insufficient experimental evidence.

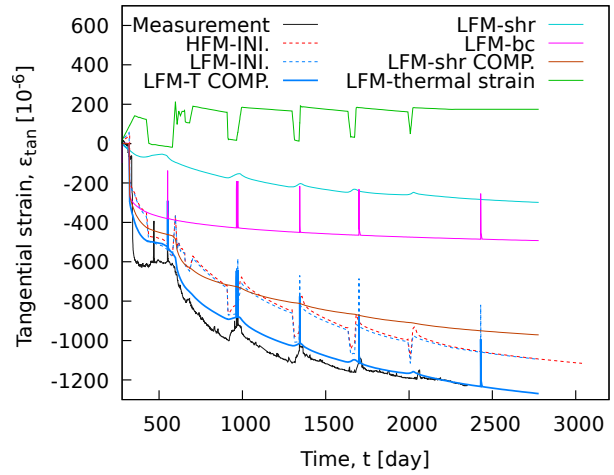


FIGURE 11. Evolution of hoop strain close to the inner face of the wall.

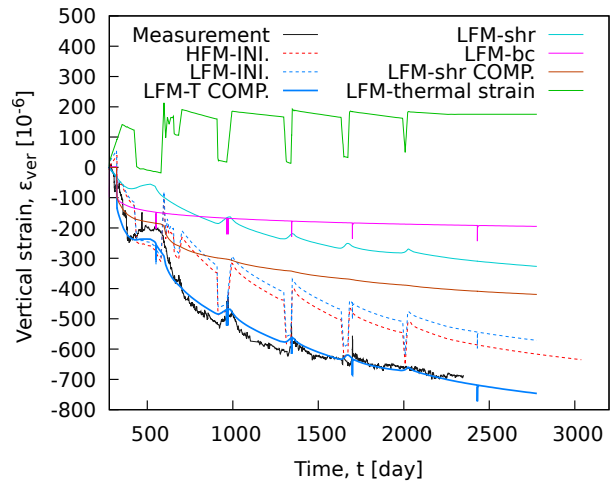


FIGURE 12. Evolution of vertical strain close to the outer face of the wall.

4.1. RELATIVE HUMIDITY

Figure 10 compares the computed and measured evolution of relative humidity in the middle of the concrete wall at the PACAR area. At first glance, it is apparent that the computed drying rate by both LFM and HFM is substantially faster than in the experiment. Additionally, it is striking that the measured data exhibit significant daily fluctuations which even reach 8% which is unrealistic given the position of the sensor at the wall middepth.

4.2. EVOLUTION OF THE STRAIN IN THE PACAR AREA

Figures 11 and 12 present the evolution of tangential and vertical strain. For clarity, Figure 13 shows the first 800 days in more detail.

Lines “LFM-INI.” and “HFM-INI.” represent the initial and unprocessed FEM results. There is a good agreement between HFM and LFM with only subtle differences that might be attributed to the slightly different placement of virtual sensors and/or FEM discretization. This concordance allowed to present

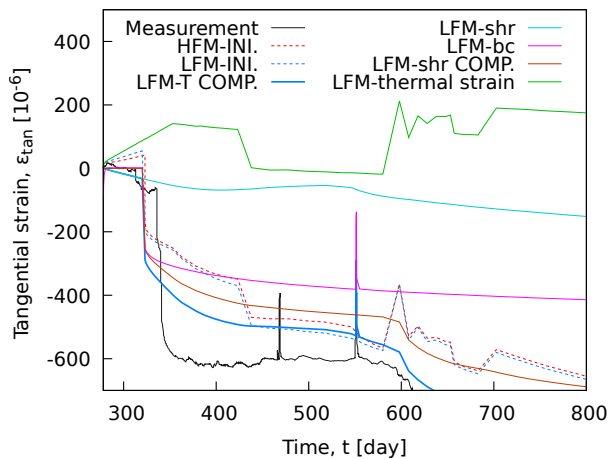


FIGURE 13. Evolution of hoop strain close to the inner face of the wall - detailed view.

the results of LFM with several modifications introduced. First, the “LFM-thermal strain” curve was computed, which represents only the strain induced by variations in ambient temperature. Subsequently, this strain was subtracted from the original “LFM-INI” curve to produce data series “LFM-T COMP” which is in very good agreement with the strains provided in the VERCORS benchmark. In the vertical direction, the prediction is almost perfect, while in the hoop direction the experimental response is initially slightly underestimated, which can be explained by overestimated prestress losses due to friction. It is of interest that even though the drying rate is overestimated (Figure 10), the structural response seems to match.

The remaining curves are added to illustrate the influence of the individual factors. Line “LFM-shr” represents only the influence of drying shrinkage (without prestressing). Basic creep of concrete and steel relaxation only were considered in “LFM-bc”. The significance of drying creep is illustrated in “LFM-shr COMP” in which both basic and drying creep were considered and the results are compensated for shrinkage (“LFM-shr”). Increased pressure during prescribed pressure tests are manifested by the spikes in the hoop strain. In the vertical direction, the spikes have opposite orientation than in the experiment; this is because no equivalent pressure was applied in the vertical direction and the response in Figure 12 is merely the consequence of the lateral pressure scaled by the Poisson-effect.

5. CONCLUSIONS

The blind prediction submitted by the present authors shows satisfactory agreement with the experimental data even though the simulation completely neglected

the construction sequence, the prestressing schedule was unknown, and the calibration of material parameters was based entirely on laboratory experiments. The low-fidelity model which represents a periodic section of the CCB wall can substitute the high-fidelity model which covers the entire CCB if the wall behavior is of interest. The computationally efficient low-fidelity model was essential for the estimation of material parameters which could not be calibrated from the laboratory experiments and subsequently for verifying the correct definition of the high-fidelity model.

Simulation results for approximately 50 sensors over the structure were submitted to EDF for evaluation. Unfortunately, the extent of accessible data provided by the benchmark organizers does not allow further research.

ACKNOWLEDGEMENTS

The authors gratefully acknowledge financial support from the Czech Science Foundation (GA ČR), project number 21-03118S, and from the Grant Agency of the Czech Technical University in Prague, project number SGS22/030/OHK1/1T/11.

REFERENCES

- [1] Š. Krátký, P. Havlásek. Benchmark VERCORS 2022: Mechanical response of the prestressed concrete containment wall to ambient conditions. *Acta Polytechnica CTU Proceedings* **34**:26–31, 2022. <https://doi.org/10.14311/APP.2022.34.0026>
- [2] Direction Production Ingeniere, EDF. Project maquette vercors, plan general, 2012.
- [3] B. Patzák. OOFEM home page, 2000. [2022-10-13]. <http://www.oofem.org>
- [4] Z. P. Bažant, L. J. Najjar. Nonlinear water diffusion in nonsaturated concrete. *Materials and Structures* **5**:3–20, 1972. <https://doi.org/10.1007/BF02479073>
- [5] Z. Bažant, P. Havlásek, M. Jirásek. Microprestress-solidification theory: Modeling of size effect on drying creep. In N. Bicanic, H. Mang, G. Meschke, R. de Borst (eds.), *Computational Modelling of Concrete Structures*, pp. 749–758. CRC Press/Balkema, EH Leiden, The Netherlands, 2014.
- [6] Štěpán Krátký. *Benchmark VERCORS 2022 – slepá predikce chování železobetonového kontejneru [in Czech; Benchmark VERCORS 2022 – blind prediction of mechanical response of reinforced concrete containment]*. Bachelor thesis, Czech Technical University in Prague, 2021.
- [7] Z. P. Bažant, S. Baweja. Creep and shrinkage prediction model for analysis and design of concrete structures: Model B3. In *Adam Neville Symposium: Creep and Shrinkage – Structural Design Effects*, pp. 85–101. 2000.